Synthesis, structural and magnetic studies on yttrium- doped Gadolinium iron garnet (GIG) nano-particles

S. S. Jadhav[a], A.V. Fulari[b], S. B. Kadam[c], V. D. Mote[d], A. B. Kadam[a*]

[a]Department of Physics, Jawahar Arts, Science and Commerce College, Andur, Tuljapur, Osmanabad, Maharashtra, 413603, India
[b]Symbiosis Centre for Nanoscience and Nanotechnology, Symbiosis International Deemed University, Pune, India
[c]Department of Physics, Ankushrao Tope College, Jalna (M.S), India.
[d]Thin Films and Materials Science Research Laboratory, Department of Physics, Dayanand Science College, Latur, Maharashtra, 413512, India

*E-mail of corresponding author: drabkadam@gmail.com

Abstract:

Yttrium (Y) - doped Gadolinium Iron Garnet (GIG) nanoparticles synthesized by sol-gel auto-combustion technique. As synthesized sample was characterized by using X-ray diffraction (XRD), field emission electron scanning microscope (FESEM). XRD pattern of the sample confirms the single phase garnet-cubic-spinel of iron garnet crystal structure. The crystallite size, lattice constant, x-ray density, and bulk density of GIG sample was investigated from XRD analysis. The significant impact of Y on structural parameters of Gadolinium iron garnet (GIG) nano-particles. FESEM image shows the prepared sample has nanostructures. FTIR result exhibit that the number of defects, which has significant influence on the magnetic properties. VSM analysis shows the Y-doped GIG nanoparticles have room temperature paramagnetic nature.

Keywords: Iron garnet; x-ray diffraction, nanostructures; FTIR; magnetic properties.

1. Introduction

Gadolinium iron oxide has significant magnetic, magneto-optic, and sensing capabilities, making it a member of a very important class of materials [1-5]. Its magneto-optic characteristics, gas sensing potential, and potential use in bubble-domain memory systems have all been investigated for $GdFeO_3$. The ferrimagnetic nature of the garnet $Gd_3Fe_5O_{12}$ has been extensively researched due to its unique magnetic and magneto-optical characteristics.

The magnetic interactions in $Gd_3Fe_5O_{12}$ are important in this context because of the relationship between the Fe and Gd sublattices. For instance, Phan et al. found that a spin disorder on the surface of $Gd_3Fe_5O_{12}$ nanoparticles caused an increase in MCE when their size was decreased [6]. Ga-doped garnet, $Gd_3Fe_5O_{12}$, was thought to exhibit significant MCE due to geometrical-magnetic frustration by Zhitomirsky [7]. The electrical and magnetic characteristics of garnet can be altered by altering the elements in each of the three lattice locations [8, 9].

Numerous techniques have been employed recently to prepare rare earth iron oxides, including sol–gel synthesis [10–11], co-precipitation [12–14], hydrothermal synthesis [15,16], and solid-state reaction [17, 18]. Since magnetic powders might exhibit unique magnetic properties, the synthesis process is important for their creation. Because of its improved homogeneity, lower synthesis temperatures, and adjustable product qualities, the sol-gel synthesis process is the most appealing of them all. Additionally, the experimental procedure is straightforward and simple to use. This paper describes the synthesis of Y-doped GIG nanoparticles using a straightforward sol–gel method. In the meantime, a thorough investigation was conducted into their components, microstructures, and magnetic characteristics.

2. Experimental details

2.1. Materials

Yttrium substituted GIG ($Gd_{3-x}Y_xFe_5O_{12}$; x = 0.5) was synthesized by sol-gel route. AR grades (Sigma Aldrich) Gadolinium (III) nitrate hexahydrate [$Gd(NO_3)_3.6H_2O$], Yttrium(III) nitrate hexahydrate[$Y(NO_3)_3 \cdot 6H_2O$], Ferric (III) nitrate nanohydrate [$Fe(NO_3)_3.9H_2O$], Citric acid monohydrate [$C_6H_8O_7.H_2O$], and ammonium hydroxide were used as starting chemicals.

2.2. Sample preparation

The Y-doped GIG precursor solution was created by weighing each nitrate in 100 milliliters of distilled water. After mixing this solution with a magnetic stirrer until it dissolved, it was heated to 90°C until a gel formed. While the sample was being mixed, its pH value remained at 7. After the gel had formed, the solution was heated to 200°C to ignite

the gel and turn it into ash. Samples were sintered at 1200°C for 10 hours after this ash was crushed for one hour. The material was ground for two hours once more in order to perform the characterizations.

2.3. Characterization

X-ray diffractometer (XRD) was used to study strucutral properties of prepared sample. The morphology of the sample was observed by high resolution transmission electron microscopy (HR-TEM, Philips CM-200) and field emission scanning electron microscopy (FE-SEM). The energy-dispersive X-ray spectroscope (EDS) was used to confirm the elemental composition in the sample. The magnetic properties were studied by using vibrating sample magnetometer (VSM) applying magnetic field of $\pm$15 kOe.

3. Results and discussions

The XRD patterns of the produced Y-doped GIG powder is displayed in Fig. 1(a). The crystal nature of the as-burnt GIG nanoparticles is revealed by the XRD patterns. XRD patterns confirm that Y-doped sample has a single garnet phase with Ia-3d symmetry. The planes that were obtained match the standard pattern (ICDD: 01-081-0131) for GIG. These planes are (321), (400), (420), (332), (422), (521), (532), (444), (640), (642), (800), (840), (842), and (644). The lattice parameter (a) is calculated by using the relation [19]:

$$a = \sqrt{\frac{\lambda^2}{4\sin^2\theta}\left(h^2+k^2+l^2\right)} \quad (1)$$

Where (h k l) are miller indices, λ is the wavelength of X-ray ($CuK\alpha_1$), θ is the angle of diffraction of the (h k l) peaks. The calculated value of lattice parameter is found to be 12.3004 Å. The average crystallite size (t) was determined using the Scherrer formula [20]:

$$D = \frac{0.91\lambda}{\beta\cos\theta} \quad (2)$$

Where λ is the wavelength of CuK_α radiation (λ=1.5406Å), β is the full width at half maximum (FWHM) and θ is the Bragg diffraction angle. The value of average crystallite size is 22.18 nm with the composition of Y in GIG. The range of crystallite size indicates that the sample is formed in nanocrystalline form. The volume of unit cell was found to be 1861.06 $(Å)^3$. The values of x-ray density and bulk density of Y-doped GIG sample are 6.4870 and 3.0892 respectively.

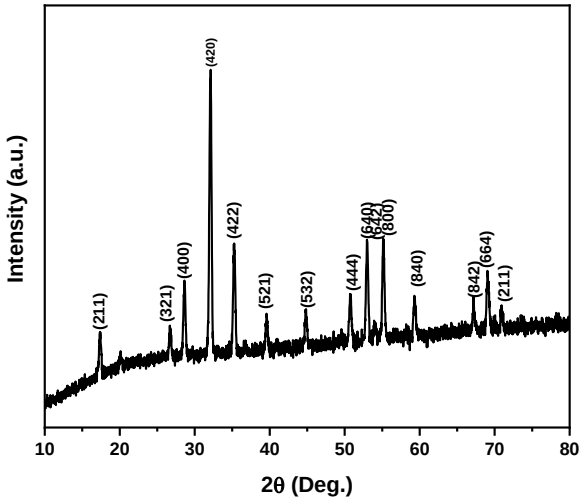

Fig. 1: XRD pattern of $Gd_{3-x}Y_xFe_5O_{12}$ (x = 0.5).

Fig. 2 shows SEM image of the Y doped sample GIG nanoparticles. The micrograph shows a similar format for the compounds; rounded irregular form. However, the Y-doped GIG sample have more porous with spherical like shape and big sized. The pore network would be useful in reducing the interactions between the nanoparticles, which would be of major significance for spintronics devices based on the previous results.

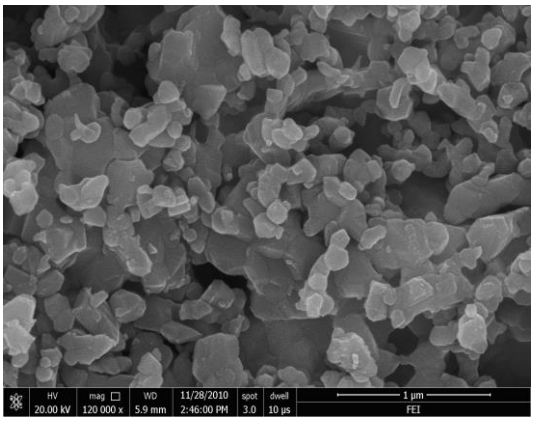

Fig. 2. SEM image for GIG doped with Y.

The FT-IR spectra of the produced $Gd_{3-x}Y_xFe_5O_{12}$ sample is displayed in Fig. 3. The FT-IR spectra of the Y-doped sample as synthesized show a few absorption peaks. A sharp absorption peaking at 541 cm^{-1} appears, and it is identified to the characteristic band of M-O (M = Y, Fe, Gd) stretching vibration mode [21].

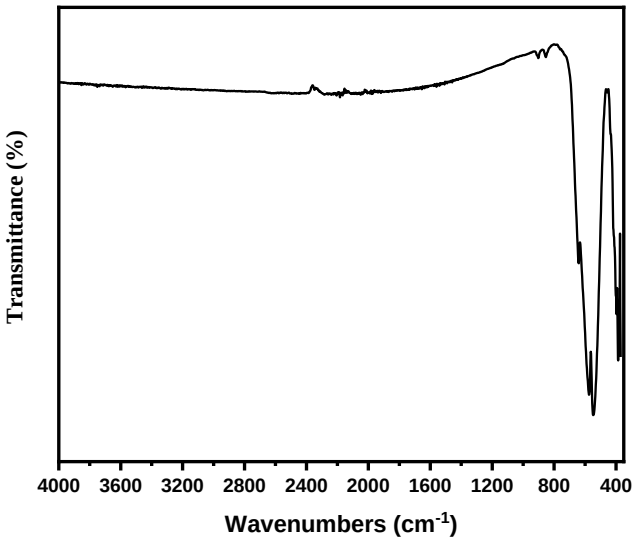

Fig. 3. FT-IR spectra of prepared $Gd_{3-x}Y_xFe_5O_{12}$ sample.

The magnetization curve at room temperature is shown in Fig. 4. The sample exhibits small hysteresis loops, which are a feature of soft magnetic materials, and low fields result in saturation magnetization (Ms). The prepared Y-doped gadolinium iron garnet (GIG) nano-particles show a soft magnetic behaviour. The enhancement in the saturation magnetization at room temperature is due to the enhanced surface area and porous materials. Furthermore, the anti-parallel coupling between two magnetic sub-lattices (octahedral (a sites) and tetrahedral (d-sites)) is known to be the cause of the total magnetic moment in GIG [22]. By decreasing the antiferromagnetic coupling from the Fe ions in the octahedral lattices, the substitution of Fe/Y in the a-sites raises the global magnetic moment and aids in a local magnetic moment rise.

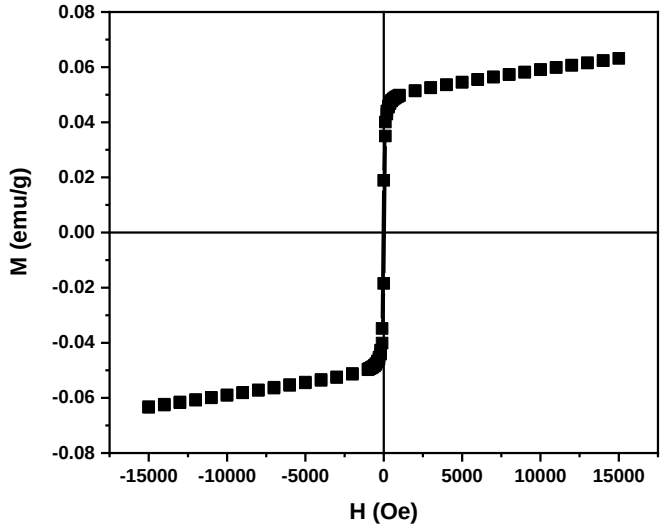

Fig. 4. Hysteresis loops of $Gd_{3-x}Y_xFe_5O_{12}$ sample.

4. Conclusions

Y-doped GIG nanocrystalline sample was prepared using by auto-combustion sol-gel method. XRD pattern exhibited single phase garnet-cubic-spinel of iron garnet crystal structure. The crystallite size of prepared samples was found to be 22.18 nm with doping of Y. The Y-doped GIG sample exhibited spherical shape, and composed of continuous porous network structure. Meanwhile, the prepared samples had big-size and agglomeration feature. The samples presented as paramagnetic feature due to the contribution of Y^{3+} paramagnetic.

References

1. S. Gokul Raj, S. Nallamuthu, R. Justin Joseyphus, Nanosci. Nanotech. Let. 3 (2011) 463-467.
2. S. Sahoo, P.K. Mahapatra, R.N.P. Choudhary, M.L. Nandagoswami, A. Kumar, Mater. Res. Express 3 (2016) 065017.
3. T. Osaka, H. Takahashi, H. Sagayama, Y. Yamasaki, S. Ishiwata, Phys. Rev. B 95 (2017) 224440.
4. X.H. Zhu, X.B. Xiao, X.R. Chen, B.G. Liu, RSC Adv. 7 (2017) 4054-4061.
5. A. Panchwanee, V. Raghavendra Reddy, A. Gupta, V.G. Sathe, Mater. Chem. Phys. 196 (2017) 205-212
6. M. H. Phan, M. B. Morales, C. N. Chinnasamy, B. Latha, V. G. Harris, and H. Srikanth, J. Phys. D: Appl. Phys. 42(11), 115007 (2009).
7. M. E. Zhitomirsky, Phys. Rev. B 67(10), 104421 (2003).
8. J. A. Quilliam, S. Meng, H. A. Craig, L. R. Corruccini, G. Balakrishnan, O. A. Petrenko, A. Gomez, S. W. Kycia, M. J. Gingras, and J. B. Kycia, Phys. Rev. B 87(17), 174421 (2013).
9. N. K. Chogondahalli Muniraju, R. Baral, Y. Tian, R. Li, N. Poudel, K. Gofryk, N. Bariˇ si´ c, B. Kiefer, J. H. Ross, Jr., and H. S. Nair, Inorg. Chem. 59(20), 15144–15153 (2020).
10. S. Zawar, S. Atiq, S. Riaz, S. Naseem, Superlattice. Microst. 93 (2016) 50-56.
11. L.S. Lobo, S. Kalainathan, A.R. Kumar, Superlattice. Microst. 88 (2015) 116-126.
12. S. Güner, S. Esir, A. Bayka, A. Demir, Y. Bakis, Superlattice. Microst. 74 (2014) 184-197.
13. V.R. Caffarena, T. Ogasawara, Mater. Res. 6 (2003) 569-576.
14. V.R. Caffarena, T. Ogasawara, M.S. Pinho, J.L. Capitaneo, Lat. Am. Appl. Res. 36 (2006) 137-140.
15. D. Aoki, M. Shima, Jpn. J. Appl. Phys. 53 (2014) 113001.
16. T. Ramesh, R.S. Shinde, S.R. Murthy, J. Magn. Magn. Mater. 324 (2012) 3668-3673.
17. L. Guo, H.M. Yuan, K.K. Huang, L. Yuan, S.K. Liu, S.H. Feng, Chem. Res. Chinese Universities 27 (2011) 715-719.
18. J.S. McCloy, B. WalshSublattice, IEEE Trans. Magn. 49 (2013) 4253-4256.
19. R.B. Borade, S.E. Shirsath, G. Vats, A.S. Gaikwad, S.M. Patange, S.B. Kadam, R.H. Kadam, A.B. Kadam, Nanoscale Adv. 1(1), 403–413 (2019).

20. Ganesan, K. P.; Anandhan, N.; Gopu, G.; Amaliroselin, A.; Marimuthu, T.; Paneerselvam, R. . (2019). Journal of Materials Science: Materials in Electronics. doi:10.1007/s10854-019-02318-5
21. S.H. Xiao, W.F. Jiang, L.Y. Li, X.J. Li, Mater. Chem. Phys. 106 (2007) 82–87.
22. Kim, T., Nasu, S., & Shima, M. (2006). Journal of Nanoparticle Research, 9(5), 737–743. doi:10.1007/s11051-006-9082-9